Phase extraction from three interferograms with different unknown tilts

Oleg Soloviev[a] and Gleb Vdovin[b]

[a]EI Lab., ITS, TU Delft, Mekelweg 4, 2628CD Delft, the Netherlands
[b]OKO Technologies B.V., P.O. Box 581, 2600AN Delft, the Netherlands

ABSTRACT

We propose an algorithm for phase retrieval from three interferograms which differ only by an arbitrary unknown tilt terms in the phase. The method is illustrated by examples.

Keywords: Interferometry,phase extraction, phase detection, interferogram analysis.

1. INTRODUCTION

In interferometry, the information about the physical quantity being measured is contained in the phase term ϕ of a fringe pattern, or an interferogram, an intensity distribution described by the formula (1). The goal of interferogram analysis[1] is to extract this phase term. The phase-shifting methods are based on general techniques of phase detection of a sinusoidal signal[2–4] and use at least three phase-shifted interferograms. The phase shifts, however, should be controlled with a high accuracy. Any error in linearity of an actuator response can introduce an error into the calculated phase. Another popular approach is based on a spatial analysis of the interferogram with discrete Fourier transform.[1, 5–7] This method needs only one interferogram, but works well only when the interferogram has a narrow bandwidth, carrier frequency and low noise level. Generally speaking, the method can not be used, if the interferogram contains closed fringes, though different techniques were proposed to deal with such interferograms.[8] Both phase-shifting and Fourier transform-based methods calculate the phase wrapped in interval $(-\pi, \pi]$. Some methods, based on local phase-tracking technique, or on genetic algorithms[9–11] return unwrapped phase values, but are computationally expensive.

This paper presents a new, to our knowledge, algorithm, which uses both spatial analysis of the interferogram and phase shifting. This allows to alleviate restriction related to the bandwidth, carrier frequency, noise level, background illumination and intensity variation, and, moreover, accuracy of phase shifts. In fact, introduced phase shifts are calculated by the algorithm, and thus are not needed to be known *a priori*. The only requirement on them is to change linearly over the detector region. Spatial analysis of two interferograms with such a phase difference detects its parameters, and then general phase-shifting algorithm is used to retrieve the phase.

2. THE ALGORITHM

We will use the following notation for an interferogram

$$I[\mathbf{x}] = a[\mathbf{x}] + b[\mathbf{x}]\cos(\phi[\mathbf{x}]), \tag{1}$$

where $\mathbf{x} = (x, y)$ denotes point position in the recorded image, and square bracket are used to emphasise its discrete nature. We assume function a and b be dependent only on the detector point position $\mathbf{x}$. Sometimes we will omit the argument $\mathbf{x}$ to facilitate the formulae reading.

Please send correspondence to Oleg Soloviev
by e-mail (preferably) O.Soloviev@EWI.TUDelft.nl
or by phone: +31 15 2786285

Opto-Ireland 2005: Imaging and Vision, edited by Fionn D. Murtagh,
Proceedings of SPIE Vol. 5823 (SPIE, Bellingham, WA, 2005)
0277-786X/05/$15 · doi: 10.1117/12.606597

Our method starts with recording three interferograms I_0, I_1, I_2, which differ from each other only by small linear term in phase, so

$$\begin{aligned} I_i[\mathbf{x}] &= a + b\cos(\phi_i[\mathbf{x}]), \quad i = 0, 1, 2, && \text{(2a)} \\ \phi_1[\mathbf{x}] &= \phi_0[\mathbf{x}] + \tau_1[\mathbf{x}] + \sigma_1, && \text{(2b)} \\ \phi_2[\mathbf{x}] &= \phi_0[\mathbf{x}] + \tau_2[\mathbf{x}] + \sigma_2, && \text{(2c)} \end{aligned}$$

where $\tau_i[\mathbf{x}] = \mathbf{t}_i \cdot \mathbf{x}$ are tilt terms and σ_i are pistons. The interferograms can be obtained, for instance, by tilting the reference mirror in Twyman-Green interferometer by a small random angle. Again we assume, that due to low dependence of a and b on phase they can be considered to be the same for all three interferograms.

For every pixel with coordinates $\mathbf{x}$ we have now three equations (2), and we have five unknowns to define: $a, b, \phi_0, \delta_1 = \tau_1 + \sigma_1, \delta_2 = \tau_2 + \sigma_2$. In phase shifting interferometry δ_1 and δ_2 are known, and equations (2) can be solved for every pixel to obtain the (wrapped) phase ϕ_0. For instance, the following identity:

$$(I_1 - I_2)\cos\phi + (I_2 - I_0)\cos(\delta_1 + \phi) + (I_0 - I_1)\cos(\delta_2 + \phi) = 0$$

can be used to find the phase as

$$\phi = \arctan\frac{I_2 - I_1 + (I_0 - I_2)\cos\delta_1 + (I_1 - I_0)\cos\delta_2}{(I_0 - I_2)\sin\delta_1 + (I_1 - I_0)\sin\delta_2}. \tag{3}$$

In our case the phase shifts δ_1 and δ_2 are supposed to be unknown and different for every pixel. Moreover, for some pixels one of the phase shifts or both of them are equal or close to integer numbers of 2π, thus reducing the numbers of equations in system (2) from three to two or one. However, as it will be shown later, for the rest of points the set of three interferograms contains enough information to determine the tilt and piston terms, and thus to make system (2) solvable.

The following method is proposed to find unknown terms. Consider the differences of interferogram $I_{d,1}$ and $I_{d,2}$:

$$I_{d,1} = I_1 - I_0 = b(\cos(\phi + \tau_1 + \sigma_1) - \cos(\phi))$$

and

$$I_{d,2} = I_2 - I_0 = b(\cos(\phi + \tau_2 + \sigma_2) - \cos(\phi)),$$

which we can write as

$$\begin{aligned} I_{d,1} &= -2b\sin\frac{\tau_1 + \sigma_1}{2}\sin\left(\phi[\mathbf{x}] + \frac{\tau_1 + \sigma_1}{2}\right), && \text{(4a)} \\ I_{d,2} &= -2b\sin\frac{\tau_2 + \sigma_2}{2}\sin\left(\phi[\mathbf{x}] + \frac{\tau_2 + \sigma_2}{2}\right). && \text{(4b)} \end{aligned}$$

Then the set of zero-crossing points for every of the differences consists of two sets: first one is due to a term $\sin\frac{\tau_i+\sigma_i}{2}$, when $\tau_i + \sigma_i = 2k\pi$, and second contains points where $\phi + \frac{\tau_i+\sigma_i}{2} = 2k\pi$, where k is an integer. The first set is not dependent on a, b, ϕ and forms parallel lines. It can be fully characterised by three parameters

$$\theta,\ \lambda,\ s, \tag{5}$$

where θ is the common normal, λ is the separation distance, and s is the distance from the origin of these lines. The algorithm proceeds by finding these parameters. Then $\mathbf{t}$ can be found as $\frac{2\pi}{\lambda}(\cos\theta, \sin\theta)$ and $\sigma = \frac{2\pi s}{\lambda}$. This gives the phase shift values δ_i for every pixel which can be substituted in equations (2) or directly in the phase formula (3).

Next section dwells on practical implementation of the algorithm and describes the method of extracting tilt and piston values from the set of zero-crossing points.

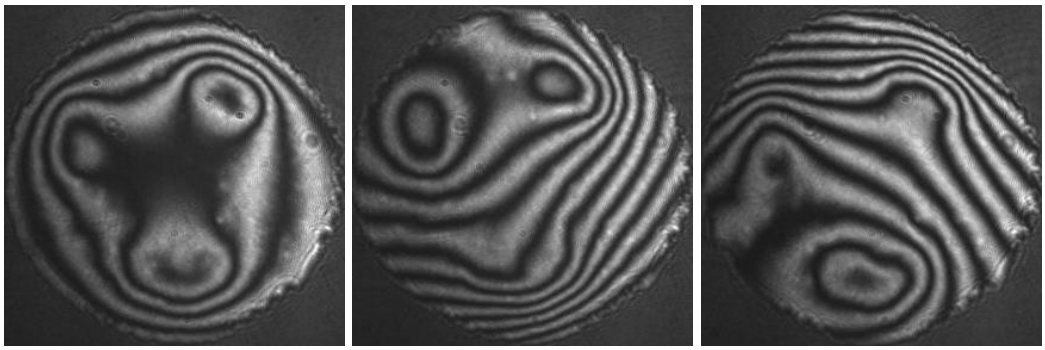

Figure 1. Three original interferograms that were obtained with a Twyman-Green interferometer. The first interferogram corresponds to original shape of a deformable mirror, additional tilts were introduced in the second and third interferograms by slightly rotating the mirror. Note that all three interferograms contain closed fringes.

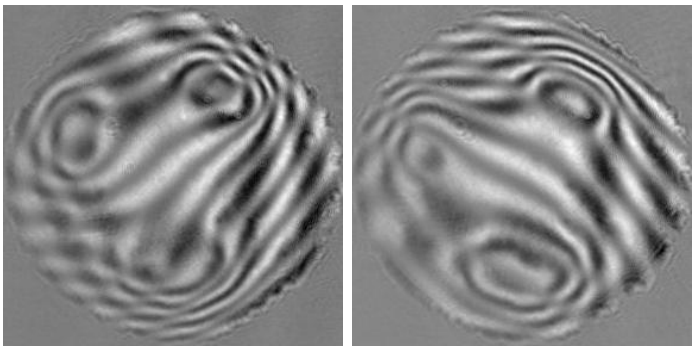

Figure 2. Differences of the interferograms $I_1 - I_0$ and $I_2 - I_0$. Black and white colours correspond to minimum (-255) and maximum (255) levels respectively.

3. PRACTICAL IMPLEMENTATION OF THE ALGORITHM AND EXAMPLES

To explain the algorithm, we describe and illustrate one of its possible implementations step-by-step. We start with the interferograms shown on Fig. 1. Subtracting interferograms, we receive following images, shown on Fig. 2. Note the regions of the middle gray level, corresponding to zero values in interferogram differences.

To extract the zero-crossing lines we have used threshold-based method – the point is considered to be zero-crossing if its value is closer to zero then some chosen value. Fig. 3 shows the zero lines extracted on this step. Points extracted from each of the interferogram difference form two sets – one with parallel lines and another repeating the fringes of half-tilted interferogram.

To determine the angle of parallel lines, their separation and shift relative to origin, we have used an algorithm based on the Hough transform.[12] The Hough transform maps any point (x, y) into a sinusoidal function $\rho = x\cos\theta + y\sin\theta$. The key property of the Hough transform is that sinusoidals in Hough space associated with points lying on the same line have a common point of intersection (ρ_0, θ_0), say. This line has a normal $(\cos\theta_0, \sin\theta_0)$ and is shifted by distance ρ_0 from the origin.

In practice, the Hough space is limited to $(\rho, \theta) \in [-R, R] \times [0, \pi)$ for some R (maximum distance of image points from the origin). Then it is quantized with finite steps $\delta_\rho = \frac{R}{m}$ and $\delta_\theta = \frac{\pi}{n}$ and is represented by matrix of size $(2m + 1) \times n$

$$\mathbf{A} = \big(A_{i,j}\big), \quad i = -m, \ldots, m,\ j = 0, n-1,$$

which is called accumulator. The rows of $\mathbf{A}$ represent the angle θ, and the columns – the radius-vector ρ. The sinusoidals for every feature pixel in Fig. 3 are "drawn" in accumulator as follows. Initially, every cell of the

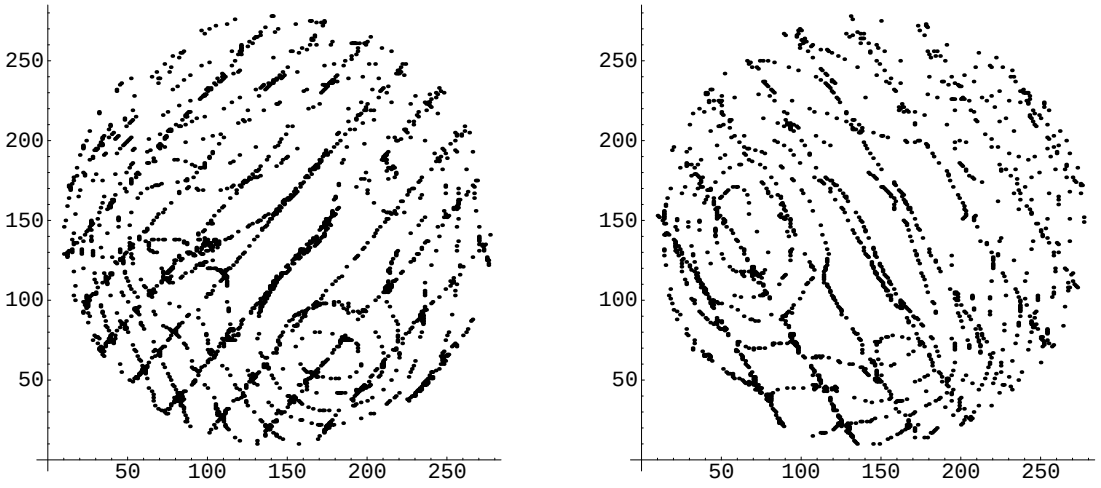

Figure 3. Points in interferogram differences which are close to zero are used as zero levels. The threshold was chosen to be 1.

accumulator is set to zero. Then for every row number j the column number $i_{(x,y)}(j)$ is calculated by

$$i_{(x,y)}(j) = \left[\frac{x\cos(j\delta_\theta) + y\sin(j\delta_\theta)}{\delta_\rho} - \frac{1}{2} \right],$$

where square brackets denote the integer part. The element $A_{i_{(x,y)}(j),j}$ is then incremented by one. The result of the Hough transform is shown on Fig. 4. The points of intersection of large number of sinusoidals are clearly visible. They all lie at row corresponding to $\theta = \pi 31/40$, as one can see on the zoomed part of the accumulator.

After the Hough transform is calculated, the parameters (5) are found as follows. Find the maximum element M in the $\mathbf{A}$ and use θ_M and ρ_M corresponding to its position as lines normal θ and shift from origin s. To find the separation distance λ, consider the row of the accumulator corresponding to θ_M (Fig. 5), and find the average distance between its local maxima, which have values greater then αM for some threshold α (typical values are

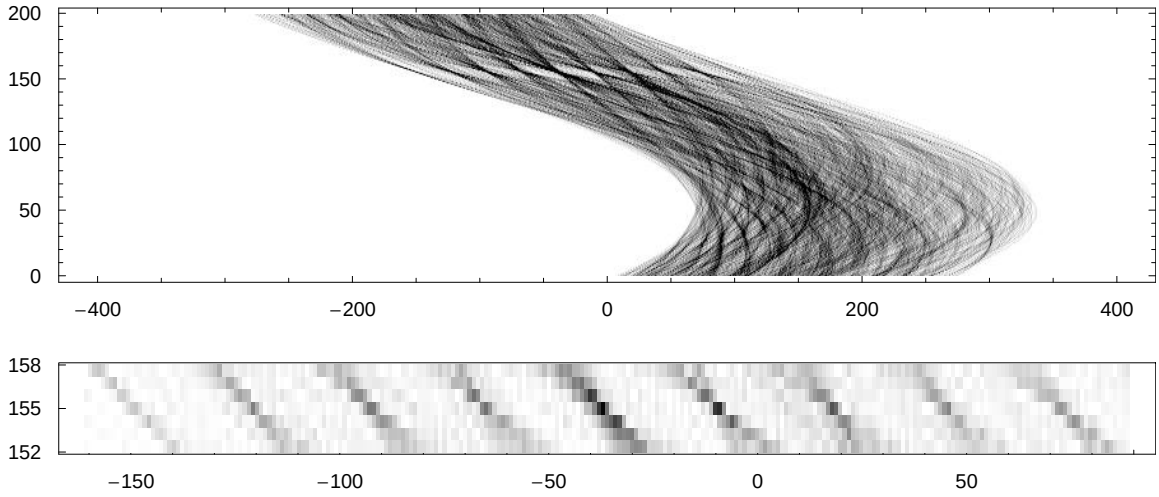

Figure 4. The interferogram difference $I_{d,1}$ in the Hough space.$R = 410$, $\delta_\rho = 1$, $\delta_\theta = \pi/200$. The second picture represents the part of the accumulator near the intersection points.

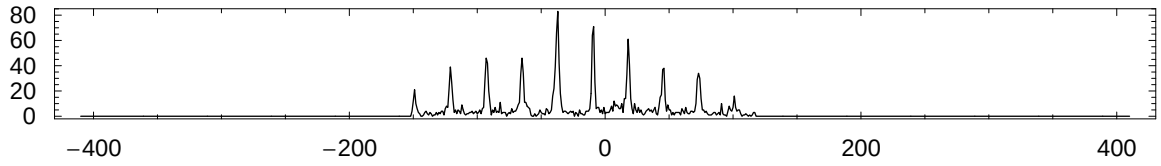

Figure 5. Accumulator's row containing the maximum element. The local maxima corresponds to the sinusoidal intersection points. The highest maxima corresponds to parallel lines in zero-crossing curves.

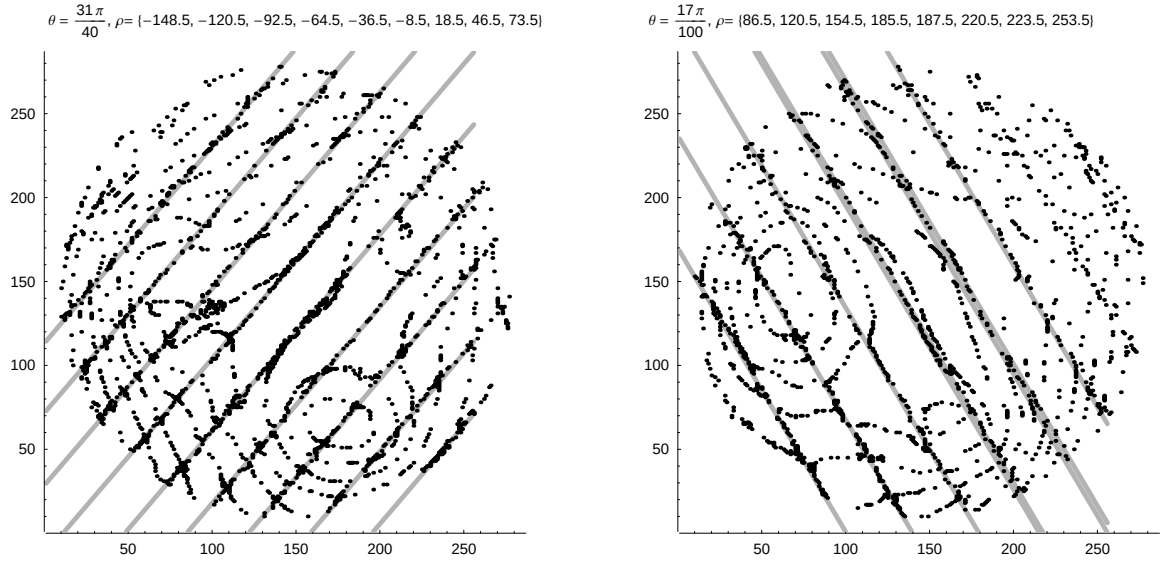

Figure 6. Lines detected by the Hough transform. The threshold α for maxima selection was set to 1/5 for the first zero-level points set and to 2/5 for the second one.

$0,3-0,7$, see Fig. 6). To reduce influence of the noise algorithm replaces nearby positioned maxima with their average.

To test the found values for the added tilts one can divide interferogram differences (4) by the first term $-2\sin\frac{\tau_i+\sigma_i}{2}$, to obtain

$$\hat{I}_{d,1} = b\sin\Big(\phi[\mathbf{x}]+\frac{\tau_1+\sigma_1}{2}\Big) \quad \text{and} \tag{6a}$$

$$\hat{I}_{d,2} = b\sin\Big(\phi[\mathbf{x}]+\frac{\tau_2+\sigma_2}{2}\Big), \tag{6b}$$

shown on Fig 7. With proper values of the tilt the picture should be as smooth as original interferogram except the vicinities of the parallel lines, were $\sin\frac{\tau_i+\sigma_i}{2}$ is close to zero.

Now the phase ϕ can be found. Instead of formula (3) one can use simpler identity

$$\sin(\phi+\alpha)=\cos(\phi+\beta)\sin(\alpha-\beta)+\cos(\alpha-\beta)\sin(\phi+\beta)$$

to write

$$\cos(\phi+\beta)=\frac{\sin(\phi+\alpha)-\cos(\alpha-\beta)\sin(\phi+\beta)}{\sin(\alpha-\beta)}.$$

Thus one can obtain, with $\alpha=\delta_1/2=\frac{\tau_1+\sigma_1}{2}$ and $\beta=\delta_2/2=\frac{\tau_2+\sigma_2}{2}$,

$$b\cos\Big(\phi[\mathbf{x}]+\frac{\tau_2+\sigma_2}{2}\Big)=\frac{\hat{I}_{d,1}-\cos(\frac{\tau_1+\sigma_1-\tau_2-\sigma_2}{2})\hat{I}_{d,2}}{\sin(\frac{\tau_1+\sigma_1-\tau_2-\sigma_2}{2})}. \tag{7}$$

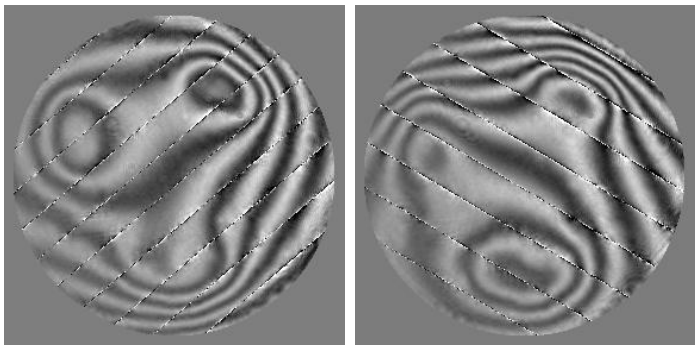

Figure 7. Interferogram differences divided by $-2\sin\frac{\tau_i+\sigma_i}{2}$.

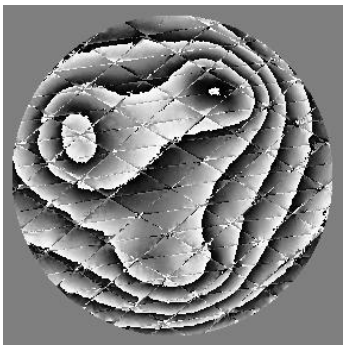

Figure 8. Extracted phase $\phi+\frac{\tau_2+\sigma_2}{2}$.

This together with (6b) permits to calculate the phase $\phi+\delta_2/2$ as

$$\phi+\frac{\tau_2+\sigma_2}{2}=\arctan\Big(\frac{\hat{I}_{d,1}-\cos(\frac{\tau_1+\sigma_1-\tau_2-\sigma_2}{2})\hat{I}_{d,2}}{\sin(\frac{\tau_1+\sigma_1-\tau_2-\sigma_2}{2})},\hat{I}_{d,2}\Big)\,. \tag{8}$$

The result is presented on Fig. 8.

4. DISCUSSION

This section gives some remarks on the algorithm and its applicability.

4.1. Artefacts in the extracted phase

Extracted phase on Fig. 8 contains visible errors along the lines where either δ_1, or δ_2, or $\delta_1-\delta_2$ is equal to $2k\pi$, $k\in\mathbb{Z}$, that is where the system (2) is badly defined. Though these artifacts introduce small rms error, they can seriously affect the unwrapped phase. They can be removed either by introducing fourth interferogram with tilt δ_3 in the algorithm, and calculating the phase as median of the results of three possible tilt combinations; or by obtaining a and b from the system (2), and then calculating the phase ϕ by substituting their smoothed by low-pass filter in equation (1); or just by using robust and noise immune phase unwrapping algorithms.

4.2. Initial phase

If the phase originally has a large linear carrier, its fringes are close to the set of parallel lines themselves, and this can interfere with phase shift detection. In this case some initial estimates on introduced tilts are needed.

4.3. Optimal tilt range

As the tilt information is derived from spatial analysis based on periodicity, it should change at least several wavelengths over the detector area. The more lines are contained in the zero-level points, the more accurate are the calculated parameters (5). On the other side, for large tilts the zero-level points due to the second terms in (4) begin to approach parallel lines with the same slope, making the tilt detection difficult. Thus the algorithm works best for those tilt values, where Fourier-transform base methods fail.

4.4. Computational effectiveness

The accuracy of the extracted tilts is dependent on the angle and radius resolution of the accumulator. To fill the accumulator with angle step $\delta_\theta = \pi/n$ one need $O(n \times N)$ operations, where N is the number of points in zero-level set. To speed up the calculation it is better to estimate first the tilt with lower resolution, and then fill only the small region of accumulator near the maximum with high resolution.

4.5. Robustness

The algorithm is not dependent on a and b as long as they are the same for all the interferograms. In regions where b is close to zero or in case of high noise level of the detector spurious zero-level points appears and decrease the accuracy. The algorithm also fails for overexposed interferograms.

5. CONCLUSIONS

We have presented a new algorithm for phase retrieval from three interferograms which differ by unknown tilt terms in the phase. The method does not require presence of carrier frequency or exact control of the phase shifts. We tested algorithm with real data and obtained good results. The method can be used in applications which use inexpensive or non-linear actuators or control system.

REFERENCES

1. D. Malacara, M. Servín, and Z. Malacara, *Interferogram analysis for optical shop testing*, Marcel Dekker, Inc., New York, Basel, Hong Kong, 1998.
2. Y. Surrel, *Photomechanics*, ch. Fringe analysis, pp. 55 –102. Springer, 1999.
3. Y. Surrel, "Design of algorithms for phase measurements by the use of phase stepping," *Applied Optics* **35**, pp. 51 – 60, 1 January 1996.
4. D. Malacara, ed., *Optical Shop Testing*, John Wiley & Sons, Inc., 2nd ed., 1992.
5. T. Kreis, "Digital holographic interference-phase measurement using the fourier-transform method," *J. Opt. Soc. Am. A* **3**, pp. 847–855, June 1986.
6. J. A. Quiroga, J. A. Gómez-Pedrero, and Á. García-Botella, "Algorithm for for fringe pattern normalisation," *Optics Communications* **197**, pp. 43–51, 2001.
7. C. Roddier and F. Roddier, "Interferogram analysis using fourier transform techniques," *Appled Optics* **26**, pp. 1668–1673, 1987.
8. Z. Ge, F. Kobayashi, S. Matsuda, and M. Takeda, "Coordinate-transform technique for closed-fringe analysis by the fourier-transform method," *Applied Optics* **40**, pp. 1649–1657, April 2001.
9. F. Cuevas, J. Sossa-Azuela, and M. Servin, "A parametric method applied to phase recovery from a fringe pattern based on a genetic algorithm," *Optics Communications* **203**, pp. 213–223, March 2002.
10. M. Servin, J. A. Quiroga, and J. L. Marroquin, "General n-dimensional quadrature transform and its application to interferogram demodulation," *J. Opt. Soc. Am. A* **20**, pp. 925–934, May 2003.
11. E. Yu and S. S. Cha, "Two-dimensional regression for interferometric phase extraction," *Applied Optics* **37**, pp. 1370–1376, March 1998.
12. G. X. Ritter and J. N. Wilson, *Handbook of computer vision algoritm in image algebra*, CRC Press, Boca Raton, New York, London, Tokyo, 1996.